

Hamburger Beiträge

zur Angewandten Mathematik

Clifford Algebras and Dimensionality Reduction for Signal Separation and Classification

Mijail Guillemard, Armin Iske, and Udo Zölzer

Nr. 2010-04
April 2010

CLIFFORD ALGEBRAS AND DIMENSIONALITY REDUCTION FOR SIGNAL SEPARATION AND CLASSIFICATION

Mijail Guillemard^{1,2}, Armin Iske¹, and Udo Zölzer²

¹University of Hamburg, Department of Mathematics, 20146 Hamburg, Germany

² Helmut-Schmidt-University, Department of Signal Processing, 22043 Hamburg, Germany

ABSTRACT

The challenging task of separating or extracting components from a signal has multiple applications in biomedical signal analysis, speech and musical acoustics, or image processing. Fourier analysis, wavelet transforms and frame theory are powerful tools for addressing these problems. However, due to the high complexity of many real-world signals, more sophisticated analysis methods are essentially required. During the last few years, there has been a strong development in data analysis using concepts from differential geometry and algebraic topology for analyzing the dimensionality reduction problem of high-dimensional data. In this paper, we propose a novel approach for signal separation and classification combining standard signal processing tools with geometric algebra and dimensionality reduction. Our concept relies on geometrical transformations, defined in the context of Clifford algebras, for modifying the geometry of a point cloud data. The objective is to transform signal components to elements of an orthonormal basis, where filtering procedures can be applied. This new framework is an addition to the manifold learning and dimensionality reduction toolbox, combining ideas from Clifford algebras, dimensionality reduction, cluster analysis via persistent homology, and filtering procedures in signal analysis. Some computational experiments ¹ are presented indicating the potential and shortcomings of this framework.

Index Terms— signal separation, STFT wavelets frame theory, dimensionality reduction, Clifford algebras, geometric algebra, Möbius transforms, radial basis functions, cluster analysis and persistent homology.

1 Introduction and Overview

In the field of signal separation, a fundamental strategy is the usage of Fourier transforms or wavelet analysis for filtering particular components of a signal. These concepts provide a powerful framework used in multiple

theoretical and application fields. But the ever increasing complexity of signal data requires more sophisticated analysis tools. In the last decade, significant progress has been made in the field of data analysis and dimensionality reduction inspired by geometrical and topological concepts [6]. New algorithms based on differential geometry are Whitney embedding based methods, Isomap, LTSA, Laplacian eigenmaps, Riemannian normal coordinates, to mention but a few. In parallel developments, probabilistic conditions and numerical algorithms (e.g. persistent homology) have provided new tools for reconstructing the homology of a manifold $\mathcal{M} \subset \mathbb{R}^n$ from a finite dataset $X = \{x_i\}_{i=1}^m \subset \mathcal{M}$. Inspired by these developments, we propose a framework based on Clifford geometry for signal separation, as an addition to the manifold learning and dimensionality reduction toolbox.

In our problem, we consider a bandlimited signal $f \in L^2([0, 1])$ and a segmentation of its domain in such a way that small consecutive signal patches are analyzed, as routinely performed in STFT or wavelet analysis. For instance, the set of signal patches can be defined as a dataset

$$X_f = \{x_i^f\}_{i=1}^m, \quad x_i^f = (f(t_{k(i-1)+j}))_{j=0}^{n-1} \in \mathbb{R}^n,$$

for $k \in \mathbb{N}$ a fixed hop-size. Here, the regular sampling grid $\{t_\ell\}_{\ell=0}^{km-k+n-1} \subset [0, 1]$ is constructed when considering the Nyquist-Shannon theorem for f . Now, a standard signal separation problem is to remove from f a component x_σ that appears at different time positions t , with varying frequency characteristics. Note that many relevant application problems dealing with a mixture of signals can be considered in this setting. For instance, in *noise reduction* we have a perturbation of a signal f by nonstationary noise σ . A typical non-blind solution scenario is to select a patch x_σ of sufficient noise characteristics such that an adequate removal can be performed (for instance using spectral subtraction methods). A more complex situation are *cocktail party effect* problems, where $f = g + h$ is a mixture of two signals g and h , and the objective is to separate g and h from f (classically

¹Available at www.math.uni-hamburg.de/home/guillemard/clifford/

addressed with independent component analysis in multichannel signals). For the sake of simplicity, we restrict ourselves to the situation where some knowledge of X_g and X_h is given (e.g. in form of representative patches $x_g \in X_g, x_h \in X_h$). Moreover, for a signal transformation T (identity, Fourier, power spectrum, wavelet, etc), and $T(X) := \{T(x_i)\}_{i=1}^m$, we consider the case where $T(X_g)$ or $T(X_h)$ are localized in small regions of \mathbb{R}^n and the size of $T(X_g) \cap T(X_h)$ is negligible. A concrete acoustical example is a one-channel signal f composed of two different percussion instruments (g and h). It is reasonable to obtain sample patches $x_g \in X_g$ and $x_h \in X_h$, but due to their complex frequency characteristics, an accurate separation of f , specially when g and h are played simultaneously, is a challenging problem. In the particular case of noise reduction, *power spectral subtraction* is a fundamental strategy which removes the noise signal g from $f = g + h$ by subtracting the frequency content $\|\hat{f}_k\| - \|\hat{h}_k\|$ at each frequency bin k [7]. A basic hypothesis is that the noise and clear signal vectors are orthogonal to each other. But this assumption is usually wrong, and a generalized approach takes into account a more accurate geometrical relation between the noise and signal vectors [8]. In our framework we use this generalized scenario but considering point cloud data structures instead of single frequency bins.

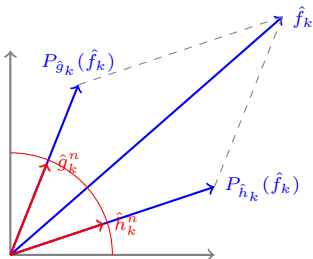


Diagram 1: Power Spectral Subtraction

1.1 General Algorithm Framework

In this section, we describe the basic ingredients of our framework. We assume we are given the dataset $X_f = \{x_i^f\}_{i=1}^m \subset \mathbb{R}^n$ sampled from a bandlimited signal $f = g + h$. We consider a signal transformation T (power spectrum, wavelet transforms, etc). Our main objective is to use the point cloud data $T(X_f)$ in order to extract the signal g from f . A fundamental component is a dimensionality reduction map R which reduces the dimension of $T(X_f)$, and provides an initial simplification of its geometry. The resulting set, $R(T(X_f)) = \Omega_f$, is further manipulated with a Möbius map \mathfrak{f} that rotates and shrinks a particular cluster (X_h or X_g). With these geometrical manipulations a filtering procedure \mathcal{T} is now implemented, extracting the signal of interest.

The crucial preprocessing step of this algorithm, is the *learning phase* which constructs the Möbius map \mathfrak{f} by considering the low dimensional representation $R(T(X_g) \cup T(X_h))$. The objective of \mathfrak{f} is to map the elements of Ω_g close to an element e_g of an orthogonal basis, while the elements of Ω_h are transformed to another region. The second component delivered by the learning phase is the filtering procedure \mathcal{T} , which depends on e_g and the geometrical modifications of \mathfrak{f} .

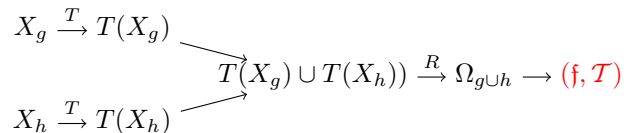


Diagram 2: Learning phase

With the resulting set $\mathfrak{f}(\Omega_{g+h})$, we can extract the contents of $g + h$ with the filter \mathcal{T} . The final step is the reconstruction of the high-dimensional data with the inverse R^{-1} in order to recover $T(X_g)$, and so g .

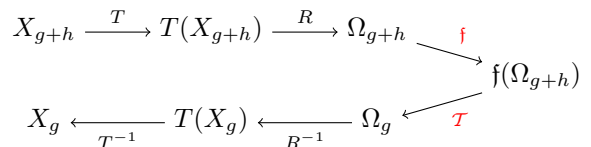


Diagram 3: Separation phase

As can be seen from this description, any gain in understanding the geometry of X_f is useful for improving the quality of the algorithm. This is particularly important since X_f may be embedded in a very high-dimensional space \mathbb{R}^n , although the dimension of X_f itself may be small (in audio analysis, for 44kHz signals, $n = 1024$ is commonly used). In such situations, customized dimensionality reduction methods are of vital interest. For instance, if $X_f \subset \mathcal{M}$, with \mathcal{M} being a manifold (or a topological space), a suitable dimensionality reduction map $R : \mathcal{M} \subset \mathbb{R}^n \rightarrow \mathcal{M}_R \subset \mathbb{R}^d$ outputs by \mathcal{M}_R a low-dimensional diffeomorphic (or homeomorphic) version of \mathcal{M} , where $d < n$. If the map R^{-1} is computationally not too expensive, then the Möbius transforms and filtering procedures in the low dimensional space $R(X_f)$ will improve the algorithmic performance.

The remainder of this paper is structured as follows. First, we briefly describe in Section 2 basic principles of dimensionality reduction. This is followed by a short description of radial basis functions as a tool for transforming data from low to high dimensions. In Section 4, we describe basic ideas of Clifford algebras as a setting for defining Möbius transforms in high dimensions. In Section 5, we discuss the potential relevance of cluster analysis with persistent homology. Finally, in Section 6, we present several computational experiments illustrating the separation and classification of signals.

2 Dimensionality Reduction

A standard way for representing experimental information is given by the concept of *point cloud data* (PCD), defined as a finite set of vectors $X = \{x_k\}_{k=1}^m \subset \mathbb{R}^n$. The *dimensional reduction* problem considers the case when much of the information described by X is redundant and can be discarded by constructing a low dimensional representation $Y = \{y_k\}_{k=1}^m \subset \mathbb{R}^d$, with $d \ll n$. The main objective is to construct a dataset Y such that certain characteristics of X are conserved. For instance, the objective in *Multidimensional Scaling* (MDS) is to find Y satisfying $\|y_i - y_j\| \approx \|x_i - x_j\|$ for all $i, j \in \{1, \dots, m\}$. Another example is the case when the dataset X lies in the vicinity of an hyperplane in \mathbb{R}^n : for this situation the goal of *Principal Component Analysis* (PCA) is to construct Y by projecting the set X in this hyperplane. The low-dimensional dataset Y can then be used for analysis or classification purposes.

In *manifold learning*, it is assumed that the elements x_i are points lying in (or close to) a manifold \mathcal{M} . We consider the case $X \subset \mathcal{M}$, namely, X is sampled from \mathcal{M} , a p -dimensional smooth compact submanifold of \mathbb{R}^n . Assuming the existence of a manifold is a reasonable hypothesis being fulfilled in relevant applications. As in dimensionality reduction, the objective is also to construct a low dimensional representation $Y = \{y_1, \dots, y_m\} \subset \mathbb{R}^d$, $d \ll n$, that conserves some characteristics of the dataset X . Now, the geometrical structure introduced by \mathcal{M} will play a crucial role in the algorithm design. Due to the Whitney embedding theorem (which states that any connected smooth p -dimensional manifold can smoothly be embedded in \mathbb{R}^{2p+1}) we require some conditions for the dimensions in this formulation, namely, $2p + 1 \leq d \leq n$. Our problem can also be formulated as the search for an adequate embedding E of the p -dimensional submanifold $\mathcal{M} \subset \mathbb{R}^n$ in \mathbb{R}^d , with $E : \mathcal{M} \subset \mathbb{R}^n \rightarrow \Omega \subset \mathbb{R}^d$, $X \subset \mathcal{M}$, $Y \subset \Omega$, Ω a p -dimensional submanifold, and $2p + 1 \leq d \leq n$.

For some applications, assuming the existence of a manifold \mathcal{M} might be too restrictive. In this case the strategy would be to construct a finite metric space from X , and analyze its properties using topological constructions, as Čech complexes, Vietoris-Rips complexes, etc (see [3]). An important additional topic in this field are density conditions on the finite dataset X (with respect to \mathcal{M}) in order to guarantee a meaningful usage of \mathcal{M} and its structure. For the case of manifolds, recent results ensuring the correct computation of the homology of \mathcal{M} using X have been presented in [9]. For more general topological spaces, the framework of *persistent homology* offers robust tools for computing homological information of \mathcal{M} using as input the finite samples $\{x_k\}_{k=1}^m$ [10].

2.1 Nonlinear Dimensionality Reduction

In order to handle point cloud data with a more complex geometry, a rich variety of algorithms have been proposed in the last few years. We describe here, as a representative example, the *Isomap* algorithm. The Isomap algorithm computes geodesic distances by considering the shortest path between groups of neighboring points. This procedure first identifies neighbor points using a k -nearest neighbors or ϵ radius criteria. Once the neighboring points are identified, the geodesic distance between two given points is computed by finding minimum connecting paths. As soon as the geodesic distances for the given dataset are obtained, the MDS algorithm can be applied: by solving an optimization problem, we construct a configuration of points Y in a lower dimensional space that matches the distances in the original dataset X . The main points are summarized in the following list of steps.

- 1 **Neighborhood graph construction:** Define a graph where each vertex is a datapoint, and each edge connects two points if they fulfill an ϵ -radius or k -nearest neighbors criterium.
- 2 **Geodesic distance construction:** Compute the geodesic distance between each pair of point using the graph by finding the shortest paths between the points.
- 3 **d -dimensional embedding:** Use the geodesic distance in a MDS algorithm for computing a d -dimensional embedding.

By using the geodesic distances we can construct a configuration of points representing a more accurate representation of the point cloud data.

2.2 Signal Processing and DR Interactions

As already explained in the outset of the introduction, it is desirable to work with analysis techniques that combine signal processing transforms with dimensionality reduction methods. In this case, the basic objects are the manifold \mathcal{M} , the data samples $X = \{x_i\}_{i=1}^m$ taken from \mathcal{M} , and a diffeomorphism $\mathcal{A} : \Omega \rightarrow \mathcal{M}$, where Ω is the low-dimensional copy of \mathcal{M} to be reconstructed via dimensionality reduction. Here, the only algorithmic input is the dataset X , but with the assumption that we can reconstruct topological information of \mathcal{M} with X (see for instance [9]). The other basic object in our scheme is a signal processing map $T : \mathcal{M} \rightarrow \mathcal{M}_T$, which may be based on Fourier analysis, wavelet transforms, or convolution filters, together with the resulting set $\mathcal{M}_T := \{T(p), p \in \mathcal{M}\}$ of transformed data. The following diagram shows the basic situation.

$$\begin{array}{ccc}
\Omega \subset \mathbb{R}^d & \xrightarrow{\mathcal{A}} & X \subset \mathcal{M} \subset \mathbb{R}^n \\
& & \downarrow \mathcal{T} \\
\Omega' \subset \mathbb{R}^d & \xleftarrow{R} & \mathcal{T}(X) \subset \mathcal{M}_{\mathcal{T}} \subset \mathbb{R}^n
\end{array}$$

The main objective is to find an approximation of Ω , denoted $\Omega' = R(\mathcal{M}_{\mathcal{T}})$, by using a suitable dimensionality reduction map R . Some properties of Ω and Ω' may differ depending on the dimensionality reduction technique, but the target is to construct Ω' , so that geometrical and topological properties of Ω are recovered. In Section 6.1, we use a particular modulation map \mathcal{A} and we study the geometrical effects being incurred by several dimensionality reduction maps $R : \mathcal{M} \rightarrow \Omega'$.

3 Radial Basis Function Interpolation

An important ingredient in our framework are radial basis functions (RBF) and their interpolation methods for high-dimensional data. As previously described in our framework (Section 1.1), our usage of dimensionality reduction requires to map data between high and low dimensional spaces. Some dimensionality reduction methods have intrinsic interpolation strategies, but in general, the reconstruction of high-dimensional data from the low-dimensional representation is a non trivial problem. In order to consider a flexible framework that embraces different reduction methods, we consider the multi-purpose features of RBFs as already suggested, for instance, in [2].

The inputs of the RBF interpolation methods are the datasets $X = \{x_i\}_{i=1}^m \subset \mathbb{R}^n$ and $Y = \{y_i\}_{i=1}^m \subset \mathbb{R}^d$. The RBF interpolant requires a family of centers $\{c_j\}_{j=1}^N$ (simply chosen randomly from the datasets in our experiments), and can be written as:

$$y_k = w_0 + \sum_{j=1}^N w_j \phi(\|x_k - c_j\|), \quad k = 1, \dots, m,$$

or in matrix form, this can be described as:

$$Y = W\Phi^T,$$

with the $m \times (N + 1)$ matrix $\Phi = (\mathbf{1}_m, \Phi_1, \dots, \Phi_N)$, $(\Phi_j)_k = \phi(\|x_k - c_j\|)$, the $d \times (N + 1)$ coefficient matrix $W = (w_0, \dots, w_N)$, and the $d \times m$ matrix $Y = (y_1, \dots, y_m)$. A solution can be constructed with the *pseudo-inverse* Φ^\dagger : $W^T = \Phi^\dagger Y^T$. In our computational experiment we use the Gaussian RBF $\phi(r) = \exp(-r^2/\alpha)$, for some fixed $\alpha > 0$.

4 The Clifford Algebra Toolbox

Another ingredient in our framework is a mechanism for manipulating the geometry of a point cloud data. For this purpose a basic building block is given by the conceptual interplay between Clifford algebras, exterior algebras, and geometric algebra. These tools can be particularly important in the design of signal separation and classification algorithms. In fact they provide efficient algebraic methods for manipulating geometrical data, and they lead to flexible nonlinear functions in high dimensional spaces. Here, we focus on the construction of a fundamental nonlinear map, the Möbius transformation in \mathbb{R}^n .

A Clifford algebra is a generalization of the complex numbers defining a product in the vector space $V = \mathbb{R}^n$ with similar properties as the complex multiplication. More precisely, let q_n be the standard Euclidean inner product in \mathbb{R}^n . Then, the Clifford algebra $\text{Cl}_n = \text{Cl}(\mathbb{R}^n, q_n)$ is an associative algebra generated by the elements of \mathbb{R}^n subject (only) to the relation $v^2 = -q_n(v, v)1, v \in \mathbb{R}^n$. More general bilinear forms q_n are of relevance in many fields (e.g. differential geometry or noncommutative geometry [5]), but here we restrict ourselves to the case of the standard inner product. An explicit construction is given by considering Cl_n to be the associative algebra over the reals generated by elements e_1, \dots, e_n subject to the relations $e_i^2 = -1, e_i e_j = -e_j e_i, i \neq j$ (anti-commutativity). Every element $a \in \text{Cl}_n$, can be represented as

$$a = \sum_J a_J e_J, \quad e_J := e_{j_1} \dots e_{j_k},$$

where each a_J is real, and the sum ranges over all multi-indices $J = \{j_i\}_{i=1}^k \subseteq \{1, \dots, n\}$ with $0 < j_1 < \dots < j_k \leq n$. Sometimes we will abuse the notation $e_\emptyset = e_0 = 1$ for the unit of the algebra Cl_n , but it is important not to confuse the unit of Cl_n , $e_0 = 1$, with the unit of the field \mathbb{R} . With this construction it is clear that $\dim(\text{Cl}_n) = 2^n$. We follow the (non standard) selection of Vahlen and Ahlfors [1], by identifying the *vectors* of \mathbb{R}^n with the elements spanned by e_0, \dots, e_{n-1} . There are three important involutions in Cl_n similar to the complex conjugation. The *main involution* defined as $a \rightarrow a'$ which replaces each e_J by $-e_J$, the *reversion* $a \rightarrow a^*$, which reverses the order of each multi-index in e_J , and their combination, the *Clifford conjugation*, $a \rightarrow \bar{a} := a'^* = a^{*'}$. An important subgroup of the Clifford algebra is Γ_n , the *Clifford group*, which is the set of invertible elements in Cl_n that can be represented as products of non-zero vectors in \mathbb{R}^n .

With our particular identification of vectors \mathbb{R}^n in Cl_n , the Clifford product xy between two vectors $x, y \in$

\mathbb{R}^n , $x = \sum_{i=0}^{n-1} x_i e_i$, $y = \sum_{i=0}^{n-1} y_i e_i$, can be written as

$$xy = \left(x_0 y_0 - \sum_{i=1}^{n-1} x_i y_i \right) e_0 + \sum_{i=1}^{n-1} (x_0 y_i + x_i y_0) e_i + \sum_{i=1}^{n-1} \sum_{j=i+1}^{n-1} (x_i y_j - x_j y_i) e_{ij}.$$

Remark 4.1. (Geometric Algebra) An algebraic structure closely related to the Clifford algebra is the *exterior algebra* (or *Grassmann algebra*), $\Lambda(V)$, generated by the elements e_1, \dots, e_n with the *wedge product* (or *exterior product*) defined by the relations $e_i \wedge e_i = 0$ and $e_i \wedge e_j = -e_j \wedge e_i, i \neq j$. Basic building blocks are the exterior products of k -vectors $\{v_i\}_{i=1}^k$, also referred as *k-blades* $v_1 \wedge \dots \wedge v_k$, and linear combinations of blades, called *multi-vectors*. A useful property of the exterior product is the efficient algebraic representation of basic geometrical entities. More precisely, if we have a k -dimensional homogeneous subspace W spanned by k vectors $\{w_i\}_{i=1}^k$, the k -blade $w = w_1 \wedge \dots \wedge w_k$ can be used to represent W as

$$x \in W \iff x \wedge w = 0.$$

For instance, if x is an element of the line spanned by $v \in V$, we have $x = \lambda v$ iff $x \wedge v = 0$. If x lies in a plane spanned by v and u , then $x = \lambda v + \gamma u$ iff $x \wedge v \wedge u = 0$. But this framework is not only restricted to homogeneous subspaces: further generalizations can be considered with the same algebraic efficiency for more elaborate geometrical objects [4]. Particularly important tools in this field are efficient algorithms (the *join* and *meet* operations) for constructing the intersection and union of subspaces.

4.1 Möbius Transforms in \mathbb{R}^n

Möbius transformations, and the general concept of conformal maps, have appeared in a wide range of theoretical and practical applications, ranging from airfoil design in aerodynamics to modern problems in brain surface conformal mapping. In this paper, we are interested in their flexible geometrical properties for designing invertible nonlinear maps with computationally efficient algebraic characteristics. Recall that a Möbius transformation is a function $f: \hat{\mathbb{C}} \rightarrow \hat{\mathbb{C}}$, with $\hat{\mathbb{C}} = \mathbb{C} \cup \{\infty\}$, of the form

$$f(z) := \frac{az + b}{cz + d},$$

where $\begin{pmatrix} a & b \\ c & d \end{pmatrix} \in \text{Mat}(2, \mathbb{C})$, with $ad - bc \neq 0$. During the last century, Möbius transforms were generalized by Vahlen, Maass, and Ahlfors to arbitrary vector spaces using Clifford algebras and Clifford groups [1]:

Definition 4.1. For the vector space $V = \mathbb{R}^n$, a Möbius transform $f: \hat{\mathbb{R}}^n \rightarrow \hat{\mathbb{R}}^n$, with $\hat{\mathbb{R}}^n := \mathbb{R}^n \cup \{\infty\}$, is defined as $f(v) = (av + b)/(cv + d)$, where the Clifford matrix $H_f := \begin{pmatrix} a & b \\ c & d \end{pmatrix} \in \text{Mat}(2, Cl_n)$ is required to satisfy the following three conditions.

- 1) $a, b, c, d \in \Gamma_n \cup \{0\}$,
- 2) $ab^*, cd^* \in \mathbb{R}^n$,
- 3) $\Delta(f) := ad^* - bc^* \in \mathbb{R}^*$.

Remark 4.2. (The Vahlen-Maass Theorem) The *Vahlen-Maass Theorem* states that the set of Clifford matrices, denoted by $\text{SL}_2(\Gamma_n)$, forms a group under the matrix multiplication. Moreover, the product $H_f H_g$ corresponds to composition of Möbius transforms $f \circ g$. The Vahlen-Maass Theorem also relates the concept of Möbius maps as composition of *similarities* and *inversions over the unit sphere*) with the Clifford matrices. The expression $\Delta(f)$ is sometimes denominated *pseudo determinant*.

4.2 An Explicit Construction

In this section, we provide a simple and explicit construction of a Möbius transform in \mathbb{R}^n , satisfying the three conditions in Definition 4.1. This yields an algorithm for designing Möbius transformations matching our specific needs, as for instance, the construction of hyperbolic transformations from two given fixed points.

Remark 4.3. (Constructing Möbius transforms in $\hat{\mathbb{C}}$) For designing a Möbius transform in $\hat{\mathbb{C}}$ such that $f(x) = u, f(y) = v, f(z) = w$ we can use the following standard construction which consist of first mapping the points x, y, z to $0, 1$ and ∞ using $f_1(x) = 0, f_1(y) = 1$, and $f_1(z) = \infty$, with

$$f_1(z) := \frac{(z-x)(y-z)}{(z-z)(y-x)}, \quad H_{f_1} := \begin{pmatrix} y-z & x(z-y) \\ y-x & z(x-y) \end{pmatrix}.$$

If we consider also a second map f_2 with $f_2(u) = 0, f_2(v) = 1, f_2(w) = \infty$, we can now construct $f := f_2^{-1} \circ f_1$ with $f(x) = u, f(y) = v, f(z) = w$, using $H_f := H_{f_2}^{-1} H_{f_1}$.

The general idea of this construction can be extended to \mathbb{R}^n , but some constraints need to be considered. The following is a particular strategy that can be used in our framework.

Lemma 4.1. Given a vector $x \in \mathbb{R}^n, n > 1$, we can construct a Möbius transform f such that $f(x) = 0, f(y) = 1$ and $f(z) = \infty$, for $y, z \in \mathbb{R}^n$ provided that the following three conditions are fulfilled:

- 1) $z_i = kx_i, i = 1, \dots, n-1$, for $k \in \mathbb{R}^*$,
- 2) $y = \alpha x + \beta z$, for $\alpha, \beta \in \mathbb{R}, \alpha + \beta = 1$,

$$3) 3(x_0 - z_0)^2 = \sum_{i=1}^{n-1} (x_i - z_i)^2.$$

Proof: Using the ideas of Remark 4.3, we analyze the three conditions in Definition 4.1. Recall that with our particular identification of \mathbb{R}^n in Cl_n we have $x = \sum_{i=0}^{n-1} x_i e_i$, $y = \sum_{i=0}^{n-1} y_i e_i$, and $z = \sum_{i=0}^{n-1} z_i e_i$. For an arbitrary triple x, y, z , the coefficients

$$\begin{aligned} a &= y - z, & b &= x(z - y), \\ c &= y - x, & d &= z(x - y), \end{aligned}$$

fulfill the first requirement in Definition 4.1. As for the second condition in Definition 4.1, we have

$$\begin{aligned} ab^* &= (y - z)(z - y)^* x^* = -(y - z)^2 x, \\ cd^* &= (y - x)(x - y)^* z^* = -(y - x)^2 z, \end{aligned}$$

and the *pseudo determinant* is given by

$$\Delta(\mathbf{f}) = ad^* - bc^* = (y - z)(x - y)(z - x).$$

Now, $(y - z)^2 x \in \mathbb{R}^n$ and $(y - x)^2 z \in \mathbb{R}^n$, if

$$\begin{aligned} (\mathbf{y} - \mathbf{z})^2 \wedge \mathbf{x} &= 0, \\ (\mathbf{y} - \mathbf{x})^2 \wedge \mathbf{z} &= 0, \end{aligned}$$

where \mathbf{x} is the non-real part of x i.e. $\mathbf{x} = \sum_{i=1}^{n-1} x_i e_i$. These two conditions can be fulfilled if we require (as described in Remark 4.1) the vector $\mathbf{y} - \mathbf{z}$ to be an element of the line spanned by \mathbf{x} , and the vector $\mathbf{y} - \mathbf{x}$ to be an element spanned by \mathbf{z} . Therefore we have $\mathbf{z} = k\mathbf{x}$, $k \in \mathbb{R}$. If we select a vector $y = \alpha x + \beta z$, $\alpha + \beta = 1$, we have

$$ad^* - bc^* = (y - z)(x - y)(z - x) = \alpha\beta(z - x)^3.$$

Now, for a vector $v = \sum_{i=0}^{n-1} v_i e_i \in \mathbb{R}^n$ we have

$$v^3 = \left(v_0^2 - \sum_{i=1}^{n-1} v_i^2 \right) e_0 + \sum_{i=1}^{n-1} \left(3v_0^2 - \sum_{i=1}^{n-1} v_i^2 \right) v_i e_i.$$

Therefore $v^3 \in \mathbb{R}$ if and only if $3v_0^2 = \sum_{i=1}^{n-1} v_i^2$, which implies that $(z - x)^3 \in \mathbb{R}$ if and only if $3(x_0 - z_0)^2 = \sum_{i=1}^{n-1} (x_i - z_i)^2$. We finally notice that by combining these conditions we also need $\mathbf{z} = k\mathbf{x}$, for $k \in \mathbb{R}^*$. ■

Note that the we can relax our above conditions on $y - z$ (resp. $y - x$). But the statement on Lemma 4.1 is sufficient for our next objective. In particular, we can now construct a variety of useful linear or nonlinear maps in \mathbb{R}^n as hyperbolic Möbius transforms based on the next proposition.

Proposition 4.1. *For a pair $u, v \in \mathbb{R}^n$, $n > 1$, and two vectors $w_i = \alpha_i u + \beta_i v$, $i = 1, 2$, with $\alpha_i + \beta_i = 1$, $\alpha_i, \beta_i \in \mathbb{R}$, there exists a Möbius transform $\mathbf{f}: \hat{\mathbb{R}}^n \rightarrow \hat{\mathbb{R}}^n$ satisfying $\mathbf{f}(u) = u$, $\mathbf{f}(v) = v$, and $\mathbf{f}(w_1) = w_2$.*

Proof: This follows as a straightforward consequence of Lemma 4.1 and the Vahlen-Maass Theorem which relates the group structure of $\text{SL}_2(\Gamma_n)$ with the composition of Möbius transforms in \mathbb{R}^n (see Remark 4.2). More precisely, following the lines of Remark 4.3, we first consider the translation \mathbf{t} , with $\mathbf{t}((u+v)/2) = 0$, followed by a rotation \mathbf{r} , such that the third condition of Lemma 4.1 is fulfilled. Now we can use Lemma 4.1 for constructing two Möbius maps $\mathbf{f}_1, \mathbf{f}_2$ with $\mathbf{f}_1(\mathbf{r}(\mathbf{t}(u))) = 0$, $\mathbf{f}_1(\mathbf{r}(\mathbf{t}(w_1))) = 1$, $\mathbf{f}_1(\mathbf{r}(\mathbf{t}(v))) = \infty$, and $\mathbf{f}_2(\mathbf{r}(\mathbf{t}(u))) = 0$, $\mathbf{f}_2(\mathbf{r}(\mathbf{t}(w_2))) = 1$, $\mathbf{f}_2(\mathbf{r}(\mathbf{t}(v))) = \infty$. Using now the Vahlen-Maass Theorem the composition $\mathbf{f} := \mathbf{t}^{-1} \mathbf{r}^{-1} \mathbf{f}_2^{-1} \mathbf{f}_1 \mathbf{t}$ is a Möbius transform and its Clifford matrix is given by $H_{\mathbf{f}} = H_{\mathbf{t}}^{-1} H_{\mathbf{r}}^{-1} H_{\mathbf{f}_2}^{-1} H_{\mathbf{f}_1} H_{\mathbf{r}} H_{\mathbf{t}}$. ■

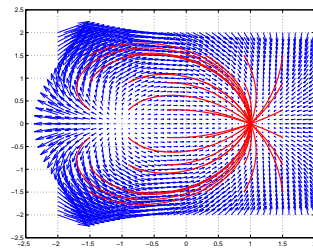


Fig. 1. Hyperbolic Möbius transform with two fixed points (one attractive and one repulsive).

By Proposition 4.1, we can now construct hyperbolic Möbius transforms by calibrating its vector field (see Fig. 1) with the vectors w_1 and w_2 . These kind of maps have useful properties for shrinking or separating clusters. In general, with Lemma 4.1 we can also design other maps, as rotations in \mathbb{R}^n , with alternative constructions to more classical strategies as the well known *Procrustes problem*.

5 Persistent Homology and Clusters

Cluster analysis is a fundamental component in the analysis of point cloud data (PCD). Recent developments in applied topology have provided robust computational and conceptual mechanisms for topological analysis of PCD [3]. For instance, the persistent homology algorithm provides qualitative information as the numbers of components, holes or voids of a PCD. This information is codified in the concept of *Betti numbers*, an algebraic topological construct characterizing a topological space by the number of unconnected components, two and three dimensional holes, (voids, circular holes), etc. Another important task we require is a hierarchical cluster analysis (dendrogram) of a PCD, together with a detection of its center components. Recent developments from applied topology have made first progress with addressing these issues, both from a conceptual and computational point of view. [3]. A basic concept relating a

given point cloud data $X = \{x_i\}_{i=1}^m$ with its topological structure is the notion of a ϵ -covering, denoted \mathbb{X}_ϵ , and defined as the union of balls $B_\epsilon(x)$ of radius $\epsilon > 0$ centered around each $x \in X$,

$$\mathbb{X}_\epsilon = \bigcup_{x \in X} B_\epsilon(x).$$

The output of the persistent homology algorithm is a barcode of intervals representing a summary of the topological information, in the form of Betti numbers, for each \mathbb{X}_ϵ , where $\epsilon \in [0, \epsilon_{\max}]$. As a straightforward application, we present in Fig. 2 the persistent barcodes for the PCD generated with the spectrogram of a corrupted speech signal. The correct interpretation and usage of persistent homology for analyzing frequency representation of signals is still work in progress, but the robust conceptual machinery of this framework is a strong motivation for a better understanding of its properties.

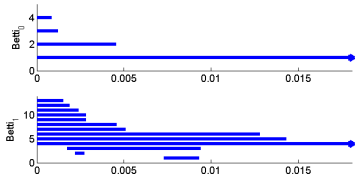


Fig. 2. Betti barcodes of a PCD spectrogram of the corrupted speech signal in the experiment of Fig. 5b.

6 Computational Experiments

In this section we present numerical examples concerning the dimensionality reduction problem using synthetic signals, based on modulation maps, and the separation and classification of speech signals.

6.1 Frequency Modulated Manifolds

We first show a basic phenomena occurring when using dimensionality reduction methods in time domain signals and their frequency representations. We present the concept of *frequency modulation manifold*, based on the standard notion of modulation techniques, but here placed in a more geometrical setting. Modulation techniques are well-known engineering procedures used to transmit data by varying the frequency content of a carrier signal. We analyze, from a dimensionality reduction viewpoint, a *frequency modulation map* $\mathcal{A} : \Omega \subset \mathbb{R}^d \rightarrow \mathcal{M} \subset \mathbb{R}^n$, where \mathcal{M} contains the carrier signals modulated by Ω . We define $\mathcal{A}_\alpha(t_i) = \sum_{k=1}^d \sin((\alpha_k^0 + \gamma \alpha_k) t_i)$, $\alpha = (\alpha_1, \alpha_2, \alpha_3) \in \Omega$, $\{t_i\}_{i=1}^n \subset [0, 1]$. The bandwidth parameter γ controls each frequency band centered at α_k^0 . The dataset to analyze (the modulated manifold) is

$\mathcal{M} = \{\mathcal{A}_\alpha\}_{\alpha \in \Omega}$, and for a Torus example $\Omega = \mathbb{T}^2$, $d = 3$, we notice the difficulty of recovering Ω with PCA, both in time and frequency domains (Figs. 3b, 4a). Isomap improves the reconstruction but still with a significant distortion (Fig. 4b). These examples were generated with $\alpha_1^0 = 1000\text{Hz}$, $\alpha_2^0 = 1200\text{Hz}$, $\alpha_3^0 = 1400\text{Hz}$, and a bandwidth of 180Hz.

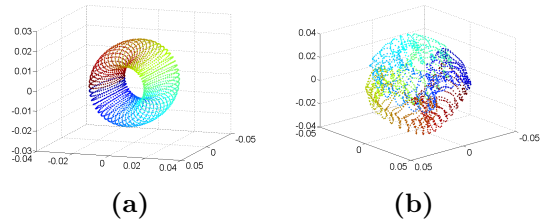


Fig. 3. (a) The torus $\Omega = \mathbb{T}^2 \subset \mathbb{R}^3$; (b) The PCA 3D projection of $\mathcal{M} = \{\mathcal{A}_\alpha\}_{\alpha \in \Omega}$.

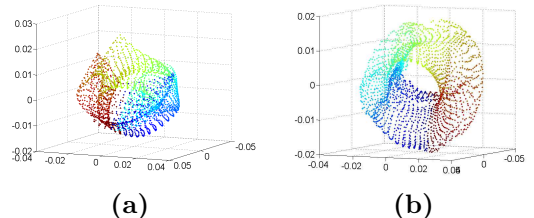


Fig. 4. (a) The PCA 3D projection of the frequency content of \mathcal{M} . (b) The Isomap 3D projection of the frequency content of \mathcal{M} .

6.2 Separation of Speech Signals

In this second set of examples, we now separate speech signals distorted with transient phenomena represented by regular clicks. Recall that we use a non-blind strategy, and a preliminary learning phase is required for storing low-dimensional clusters for the speech and click components. In the learning phase, we reduce the dimensionality of the spectrogram data (from \mathbb{R}^{128} to \mathbb{R}^8), and we design a hyperbolic Möbius transform in \mathbb{R}^8 , together with a rotational map that moves and shrinks the click cluster close to an element of the standard basis. In this case filtering procedures and projection maps can be applied. The main transformations involved are invertible, and we can then reconstruct signal data with RBF interpolation (Figs. 5,6). Despite the acoustical artifacts still present in the current prototype, these preliminary results indicate a significant potential of our method, especially since no particular parameter calibration has been implemented.

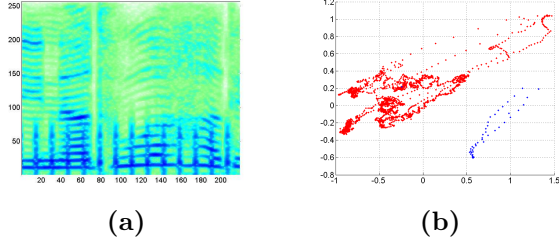


Fig. 5. (a) The spectrogram of the speech signal corrupted by regular clicks (b) The point cloud data of the speech and click signal in the learning phase.

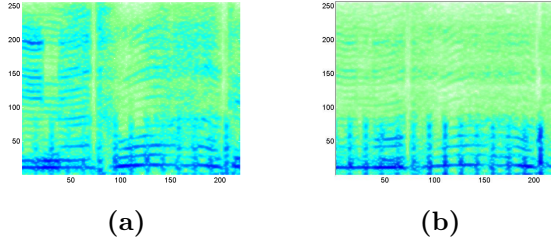


Fig. 6. (a) Extracting the speech signal (b) Extracting the clicks signal

6.3 Classification of Speech Components

Another application of our framework are classifications or identifications of consonants in a speech signal. The analysis procedures are similar to the previous example, but here no reconstruction step is required. With PCA, an identification of the consonant cluster can be achieved, but Isomap slightly improves the separation of vocal and consonant clusters, which can then be further improved with a Möbius map, designed with an attractive fixed point located in the center of the consonant cluster (Figs. 7, 8).

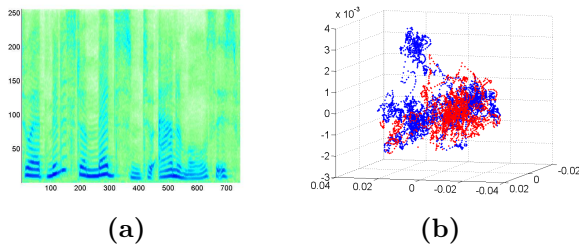


Fig. 7. (a) Spectrogram of speech signal (b) PCA projection with consonants (red) vs vocals (blue).

Acknowledgments. We would like to thank Frank Klinker for helpful conversations on Clifford algebras.

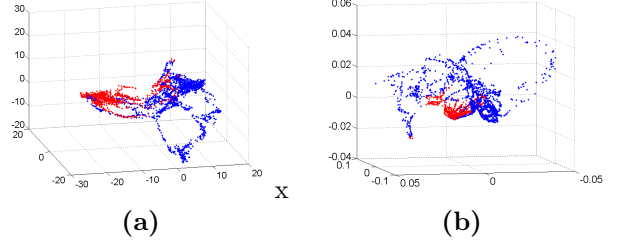


Fig. 8. (a) Isomap projection and consonants (red) vs vocal (blue) components (b) Isomap-Möbius projection.

The first and second authors are supported by the priority program DFG-SPP 1324 of the Deutsche Forschungsgemeinschaft (DFG).

7 References

- [1] L.V. Ahlfors. Möbius transformations in \mathbb{R}^n expressed through 2×2 matrices of Clifford numbers. *Complex Variables and Elliptic Equations*, 5(2):215–224, 1986.
- [2] D.S. Broomhead and M. Kirby. A new approach to dimensionality reduction: Theory and algorithms. *SIAM Journal on Applied Mathematics*, 60(6):2114–2142, 2000.
- [3] G. Carlsson. Topology and data. *American Mathematical Society*, 46(2):255–308, 2009.
- [4] L. Dorst, D. Fontijne, and S. Mann. *Geometric algebra for computer science: an object-oriented approach to geometry*. Morgan Kaufmann, 2009.
- [5] H.B. Lawson and M.L. Michelson. *Spin Geometry*. Princeton University Press, Princeton, New Jersey, 1989.
- [6] J.A. Lee and M. Verleysen. *Nonlinear dimensionality reduction*. Springer Verlag, 2007.
- [7] P.C. Loizou. *Speech enhancement: theory and practice*. CRC press Boca Raton, FL, 2007.
- [8] Y. Lu and P.C. Loizou. A geometric approach to spectral subtraction. *Speech communication*, 50(6):453–466, 2008.
- [9] P. Niyogi, S. Smale, and S. Weinberger. Finding the homology of submanifolds with high confidence from random samples. *Discrete and Computational Geometry*, 39(1):419–441, 2008.
- [10] A. Zomorodian and G. Carlsson. Computing persistent homology. *Discrete Comput. Geom.*, 33(2):249–274, 2005.